

Behavior of [S/Fe] in Very Metal-Poor Stars from the S I 1.046 μm Lines Revisited *

Yoichi TAKEDA

*National Astronomical Observatory of Japan 2-21-1 Osawa, Mitaka, Tokyo 181-8588
takeda.yoichi@nao.ac.jp*

and

Masahide TAKADA-HIDAI

*Liberal Arts Education Center, Tokai University, 4-1-1 Kitakaname, Hiratsuka, Kanagawa 259-1292
hidai@apus.rh.u-tokai.ac.jp*

(Received 2011 September 8; accepted 2011 November 7)

Abstract

With an aim of establishing how the [S/Fe] ratios behave at the very low metallicity regime down to $[\text{Fe}/\text{H}] \sim -3$, we conducted a non-LTE analysis of near-IR S I triplet lines (multiplet 3) at 10455–10459 Å for a dozen of very metal-poor stars ($-3.2 \lesssim [\text{Fe}/\text{H}] \lesssim -1.9$) based on the new observational data obtained with IRCS+AO188 of the Subaru Telescope. It turned out that the resulting [S/Fe] values are only moderately supersolar at $[\text{S}/\text{Fe}] \sim +0.2\text{--}0.5$ irrespective of the metallicity. While this “flat” tendency is consistent with the trend recently corroborated by Spite et al. (2011, A&A, 528, A9) based on the S I 9212/9228/9237 lines (multiplet 1), it disaffirms the possibility of conspicuously large [S/Fe] (up to $\sim +0.8$) at $[\text{Fe}/\text{H}] \sim -3$ that we once suggested in our first report on the S abundances of disk/halo stars using S I 10455–10459 lines (Takeda & Takada-Hidai 2011, PASJ, 63, S537). Given these new observational facts, we withdraw our previous argument, since we consider that [S/Fe]’s of some most metal-poor objects were overestimated in that paper; the likely cause for this failure is also discussed.

Key words: stars: abundances — stars: atmospheres — stars: late-type
— stars: Population II

1. Introduction

The galactic evolution of sulfur (one of the α -group elements) has been a matter of controversy, since different [S/Fe] behaviors with a decrease of [Fe/H] were suggested in the regime of metal-poor halo stars depending on the lines used; i.e., ever-increasing [S/Fe] even up to $\sim +0.8$ (S I 8693–4 lines of multiplet 6) or nearly constant [S/Fe] at a mildly supersolar value around $\sim +0.3$ (S I 9212/9228/9237 lines of multiplet 1). See, e.g., Takeda et al. (2005) and the references therein for more details.

Given this situation, we recently carried out a systematic study on the [S/Fe] ratios of 33 disk/halo stars over a wide range of metallicity ($-3.7 \lesssim [\text{Fe}/\text{H}] \lesssim +0.3$) while newly exploiting the S I triplet lines at 10455–10459 Å (multiplet 3) based on the near-IR spectra obtained with Subaru IRCS+AO188, which had barely been used before (Takeda & Takada-Hidai 2011; hereinafter referred to as Paper I). Rather unexpectedly, while the the local plateau of $[\text{S}/\text{Fe}] \sim +0.2\text{--}0.4$ (flat trend) was confirmed at $-2.5 \lesssim [\text{Fe}/\text{H}] \lesssim -1.5$ in consistent with the tendency already established from the S I 9212/9228/9237 lines (e.g., Nissen et al. 2007), we found a considerably large [S/Fe] ratio amounting to $\sim +0.7\text{--}0.8$ dex at very low metallicity ($[\text{Fe}/\text{H}] \sim -3$), which apparently makes a puzzling discon-

tinuity in the narrow interval of $-3 \lesssim [\text{Fe}/\text{H}] \lesssim -2.5$. If this trend is real, the chemical evolution of sulfur would have to be considered differently from other α elements generally showing a plateau at a mildly supersolar $[\alpha/\text{Fe}]$ over the halo metallicity range.

Soon after we published Paper I, however, Spite et al. (2011) reported new results of their extensive study on the [S/Fe] of extremely metal-poor stars, which are markedly against our conclusion (i.e., considerably high [S/Fe] at $[\text{Fe}/\text{H}] \sim -3$). That is, using the S I 9212/9228/9237 lines based on the VLT/UVES data, they showed that [S/Fe] ratio is almost constant at mildly supersolar values of $\sim 0.2\text{--}0.5$ over the very metal-poor regime of $-3.5 \lesssim [\text{Fe}/\text{H}] \lesssim -2.5$.¹ How should we interpret this discordance? Do multiplet 1 lines ($\sim 0.92 \mu\text{m}$) and multiplet 3 lines ($\sim 1.05 \mu\text{m}$) yield different S abundances at the extremely low-metallicity regime?

Yet, we need to ascertain in the first place that the trend of high [S/Fe] at $[\text{Fe}/\text{H}] \sim -3$ we obtained in Paper

* Based on data collected at Subaru Telescope, which is operated by the National Astronomical Observatory of Japan.

¹ Jönsson et al. (2011) also recently investigated the sulfur abundances of halo giants of $-2.5 \lesssim [\text{Fe}/\text{H}] \lesssim -1.5$ with the S I 10455–10459 triplet (which we used in Paper I) and the forbidden [S I] line at 10821 Å based on the VLT/CRIRES data. They then concluded that [S/Fe] favors a flat trend at $\sim +0.4$ and a high [S/Fe] (i.e., rise or scatter at low [Fe/H]) is rather unlikely. However, since the [Fe/H] range they studied is limited to between ~ -2.5 and ~ -1.5 (where we also derived a near-plateau [S/Fe]), their finding does not contradict the conclusion of Paper I.

I from the S I 10455–10459 lines universally exists for extremely metal-poor stars in general, since that conclusion was extracted from only a few objects based on the spectra of not-so-sufficient quality. We thus decided to reinvestigate the [S/Fe] behavior for a larger sample (ca. a dozen objects) specifically confined to *very* metal poor stars ($-3.2 \lesssim [\text{Fe}/\text{H}] \lesssim -1.9$) based on our new observations lately conducted again with Subaru IRCS+AO188. The purpose of this article is to report the outcome of this new analysis.

2. Observational Data

The near-IR spectroscopic observations were conducted on 2011 August 17 and 18 (UT) by using IRCS+AO188 of the Subaru Telescope for the selected 13 very metal-poor stars, among which 4 are turn-off dwarfs and 9 are evolved giants. In addition, we also observed Vesta in order to get the sun-light reference spectrum with the same equipment. The list of the targets is given in table 1. Note that G 64-37 (which was studied in Paper I) was again included in the present sample. The details of the instrument and its setting along with the data reduction procedures (the same as in our previous observations in 2009 July) are described in section 2 of Paper I.

In this observing run, a special attention was paid to achieve a sufficiently high signal-to-noise ratio so as to detect very weak S I 10455–10459 lines of extremely metal-poor stars. For this purpose, especially long integrated exposure times ($\sim 1\text{--}4$ hours) were expended to the comparatively faint ($J \sim 9\text{--}11$ mag) lowest metallicity stars ($[\text{Fe}/\text{H}] \sim -3$), such as CS 30323-048, HD 126587, G 206-34, G 64-37, HE 1523-0901, and BD-16 251. For the other brighter objects of $J \sim 5\text{--}8$ mag, we set the exposure times from a few minutes to ~ 20 min depending on the brightness. The S/N ratios, eventually accomplished in the neighborhood of the S I lines in our finally resulting zJ -band spectra (with the resolving power of $R \sim 20000$), are typically $\sim 300\text{--}500$ (cf. table 1).²

3. Analysis and Results

The atmospheric parameters (T_{eff} , $\log g$, v_t , and $[\text{Fe}/\text{H}]$) necessary for constructing the model atmosphere for each star were taken from various published studies (cf. table 1). Then, as in Paper I, the S abundance was evaluated by way of the non-LTE spectrum-synthesis analysis while applying Takeda’s (1995) automatic fitting procedure to the region of S I 10455–10459 lines.

Since we modeled the observed stellar line profile (D_{obs}) by the convolution of (i) the intrinsic spectrum (D_0 ; where only the elemental abundance A is allowed to vary since the model atmosphere and the microturbulence are given)

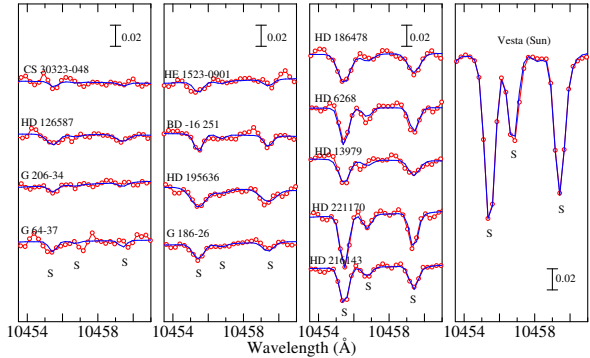


Fig. 1. Synthetic spectrum fitting for the S I 10455–10459 triplet lines. The best-fit theoretical spectra are shown by (blue) solid lines, while the observed data are plotted by (red) symbols. In each of the panels, spectra are arranged (from top to bottom, from left to right) in the ascending order of $[\text{Fe}/\text{H}]$ as in table 1. A vertical offset of 0.05 is applied to each spectrum relative to the adjacent one, and the wavelength scale has been adjusted to the laboratory frame.

and (ii) the Gaussian macro-broadening function $f_M(v)$ [$\propto \exp(-v^2/v_M^2)$] parametrized by v_M (including the combined effects of the instrumental broadening, the macro-turbulence, and the projected rotational velocity), such as $D_{\text{obs}} = D_0 * f_M$, adjustable free parameters in accomplishing the best fit are A and v_M , both of which were actually varied in the previous analysis of Paper I. However, for the reason mentioned in the next section, we intentionally *fixed* the v_M parameter in this S I 10455–10459 fitting for five extremely metal-poor stars (CS 30323-048, HD 126587, G 206-34, G 64-37, HE 1523-0901, and BD-16 251) at the pre-determined values which had been established in advance from the analysis applied to the strong C+Si feature at $\sim 1.069 \mu\text{m}$ [where $A(\text{C})$, $A(\text{Si})$, and v_M were varied to search for the best fit]. The final v_M values resulting from (or assumed as fixed in) the profile-fitting analysis are given in table 1.

How the theoretical spectrum for the converged solutions fits well with the observed spectrum is displayed in figure 1, and the resulting non-LTE S abundances (A^{N}) along with the $[\text{S}/\text{Fe}]$ values³ are presented in table 1.

In figure 2a are plotted the resulting $[\text{S}/\text{Fe}]$ ratios against $[\text{Fe}/\text{H}]$, where the abundance uncertainties (δT_{gv} ; cf. subsection 4.2 in Paper I) caused by ambiguities in T_{eff} (± 100 K), $\log g$ (± 0.2 dex), and v_t ($\pm 0.3 \text{ km s}^{-1}$) are shown by thin error bars (though they are typically on the order of $\sim \pm 0.1$ dex and not very significant).⁴ We also derived EW_{10455} (equivalent width in-

³ $[\text{S}/\text{Fe}] \equiv [\text{S}/\text{H}] - [\text{Fe}/\text{H}]$, where $[\text{S}/\text{H}] \equiv A^{\text{N}} - 7.20$. We used $A_{\odot}^{\text{N}} = 7.20$ (the value derived in Paper I based on the solar flux spectrum atlas of Kurucz et al. 1984) as the reference solar abundance in order to keep consistency with our previous study, which anyhow matches the present result (7.21; cf. table 1) derived from the spectrum of Vesta very well.

⁴ We should remark that largely different atmospheric parameters from those adopted here are reported in the literature, especially for high-gravity turn-off stars. For example, Ishigaki, Chiba, and Aoki (2010) derived (T_{eff} , $\log g$, $[\text{Fe}/\text{H}]$) of (5821,

² Actually, we noticed that some ripple patterns appeared in several restricted portion of the spectrum, which may be attributed to an imperfect flat-fielding. While this pattern was found to fall on the region of the S I lines in several cases depending on the stellar radial velocity, we could successfully remove them by dividing the spectrum by that of a rapid rotator.

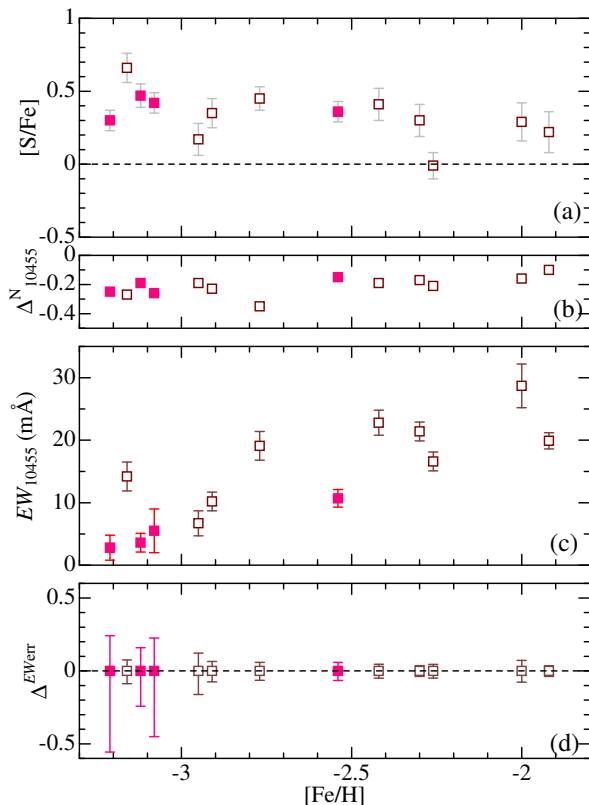


Fig. 2. Sulfur abundances and the related quantities plotted against $[\text{Fe}/\text{H}]$: (a) $[\text{S}/\text{Fe}]$ corresponding to non-LTE sulfur abundance, where attached thin error bars represent the ambiguities due to uncertainties in the atmospheric parameters ($\delta T_{\text{g}v}$; cf. subsection 4.2 in Paper I). (b) $\Delta_{10455}^{\text{N}}$ (non-LTE correction for the S I 10455 line). (c) EW_{10455} (equivalent width for the S I 10455 line) with the S/N-dependent intrinsic random error ($\pm\delta EW$) estimated from Cayrel’s (1988) formula. (d) $\Delta^{EW_{\text{err}}}$ (abundance variation in response to EW changes of $\pm\delta EW$). Dwarfs ($\log g > 3$) and giants ($\log g < 3$) are indicated by filled (scarlet) and open (brown) squares, respectively.

versely computed from A^{N} along with the corresponding non-LTE correction ($\Delta_{10455}^{\text{N}}$; negative values with typical extents of $\sim 0.1\text{--}0.3$ dex) for the strongest component (at 10455.45 Å) of the triplet in the same manner as described in subsection 4.2 of Paper I, which are given in table 1 and shown in figures 2b and 2c, respectively. The error bars (a few mÅ) accompanied with EW_{10455} in fig-

3.50, -3.66) and (6105, 3.65, -3.36) for CS 30323-048 and G 64-37, respectively, which are considerably discrepant from Nissen et al.’s (2007) results of (6338, 4.32, -3.21) and (6432, 4.24, -3.08) adopted in this study; i.e., by $\sim 300\text{--}500$ K lower in T_{eff} , by $\sim 0.6\text{--}0.8$ dex lower in $\log g$, and by $\sim 0.3\text{--}0.5$ dex in $[\text{Fe}/\text{H}]$. Interestingly, since the signs of the abundance corrections are opposite (e.g., $\delta T_{-} = +0.03$ dex for $\Delta T_{\text{eff}} = -100$ K, $\delta g_{-} = -0.06$ dex for $\Delta \log g = -0.2$ dex, for G 64-37; cf. electronic table E2 in Paper I), the net effect on $A(\text{S})$ itself is only of ~ 0.1 dex level and thus not so significant even in such extreme cases. This means, however, that $[\text{S}/\text{Fe}]$ would be appreciably raised because of the lowered $[\text{Fe}/\text{H}]$, which eventually makes a serious discordance in comparison with the $[\text{S}/\text{Fe}]$ results of other giants stars.

ure 2c are the S/N-dependent uncertainties (δEW) estimated by Cayrel’s (1988) formula, $\sim 1.6(w \delta x)^{1/2} \epsilon$, where w is the typical line FWHM ($\sim 0.5\text{--}1$ Å; assumed to be 0.75 Å), δx is the pixel size (0.25 Å), and ϵ is the photon-statistics accuracy ($\sim (\text{S}/\text{N})^{-1}$). The abundance errors ($\Delta^{EW_{\text{err}}}$) in response to these uncertainties in EW_{10455} are further displayed in figure 2d, where we can see that these errors become considerable (e.g., a few tenths dex) for extremely metal-deficient stars ($[\text{Fe}/\text{H}] \lesssim -3$) showing very weak lines ($EW_{10455} \lesssim 5\text{--}6$ mÅ).

4. Discussion

We are now ready to answer the question which motivated this study: “How do the $[\text{S}/\text{Fe}]$ ratios of very metal-poor stars behave around $[\text{Fe}/\text{H}] \sim -3$: a sudden jump to a considerably high value of $\sim +0.8$ (as suggested in Paper I) or only a mildly supersolar value at $\sim +0.4$ maintaining a flat trend (as derived by Spite et al. 2011)?” We can recognize in figure 2a that the $[\text{S}/\text{Fe}]$ ratios do not show any appreciable increase with a decrease in the metallicity, which are almost constant over $-3.2 \lesssim [\text{Fe}/\text{H}] \lesssim -1.9$ with the mean of $\langle [\text{S}/\text{Fe}] \rangle = +0.34$ ($\sigma = 0.16$) irrespective of dwarfs and giants. These $[\text{S}/\text{Fe}]$ values of very metal-deficient stars resulting from this study are combined with those of halo/disk stars derived in Paper I on the $[\text{S}/\text{Fe}]$ vs. $[\text{Fe}/\text{H}]$ plot displayed in figure 3, from which we can state that $[\text{S}/\text{Fe}]$ ratios are almost “flat” around $\sim +0.3$ over the wide metallicity range between $[\text{Fe}/\text{H}] \sim -1$ and ~ -3 . Thus, we have to admit that Spite et al.’s (2011) argument actually represented the truth, which (in turn) means that our previous conclusion of Paper I was not correct, as far as the run of $[\text{S}/\text{Fe}]$ around the regime of $[\text{Fe}/\text{H}] \sim -3$ is concerned. From an impartial point of view, however, this is a gratifying consequence in a sense, because the different abundance indicators (S I 9212/9228/9237 and S I 10455–10459) eventually turned out to yield consistent results with each other.

Then, how should we interpret the prominently high $[\text{S}/\text{Fe}]$ results once obtained for all three most metal-poor stars around $[\text{Fe}/\text{H}] \sim -3$ among the sample in Paper I; i.e., ($[\text{S}/\text{Fe}], [\text{Fe}/\text{H}]$) = ($+0.69, -3.08$) [G 64-37], ($+0.76, -3.06$) [BD-18 5550], and ($+0.66, -2.71$) [HD 115444]? With an intention to confirm whether or not these results are really reliable, we reexamined the process of the previous analysis for these stars.

Regarding BD-18 5550 and HD 115444, we noticed that the solutions of v_{M} (macrobrodening parameter; cf. section 3) resulting as by-products of spectrum fitting are unusually high (18.6 and 19.4 km s $^{-1}$, respectively) compared to other stars where values around ~ 10 km s $^{-1}$ are in common.⁵ However, additional spectrum fitting

⁵ We can roughly make an order-of-magnitude estimate of v_{M} including three kinds of macrobrodening [instrumental profile broadening (v_{ip}), macroturbulence broadening (v_{mt}), and rotational broadening (v_{rt})] based on a simple modeling, where all three broadening functions are assumed to be Gaussian and each of these parameters are the corresponding e -folding width, between which the following relation holds: $v_{\text{M}}^2 =$

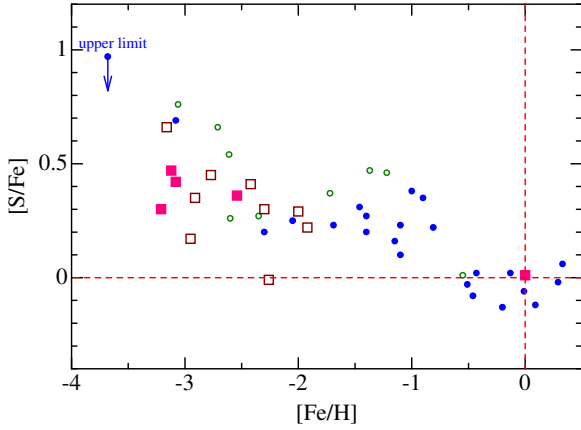


Fig. 3. $[S/Fe]$ vs. $[Fe/H]$ relation based on the results in obtained this study (larger squares) combined with those derived in Paper I (smaller circles). As in figure 2, open and filled symbols are for giants ($\log g < 3$) and for dwarfs ($\log g > 3$), respectively.

analyses to the C+Si feature at $\lambda \sim 1.069 \mu\text{m}$ carried out for these stars yielded quite reasonable v_M values of 9.4 km s^{-1} (BD-18 5550) and 10.2 km s^{-1} (HD 115444) (cf. figures 4a and 4c). Since almost the same v_M should (in principle) result from different lines, we can not help considering that the v_M values for these two stars obtained from the S I 10455–10459 fitting in Paper I were inadequately overestimated, which we suspect may presumably related to the profile-fitting technique we adopted. That is, the automatic solution-search algorithm (Takeda 1995), which simultaneously varies several parameters to accomplish the best fit, is very efficient in case where the stellar line profiles are well defined. However, we should be careful when it is applied to the very weak-line case where noises are comparable to the signal of stellar lines, since it may yield physically meaningless solutions where profiles are appreciably damaged by noises. In such cases, v_M had better be fixed at a (more reliable) value derived from other stronger lines (such as the C+Si feature), instead of varying both $A(S)$ and v_M , which is the approach we adopted for the five most metal-poor stars in this study (cf. section 3).⁶ Accordingly, we redetermined the S

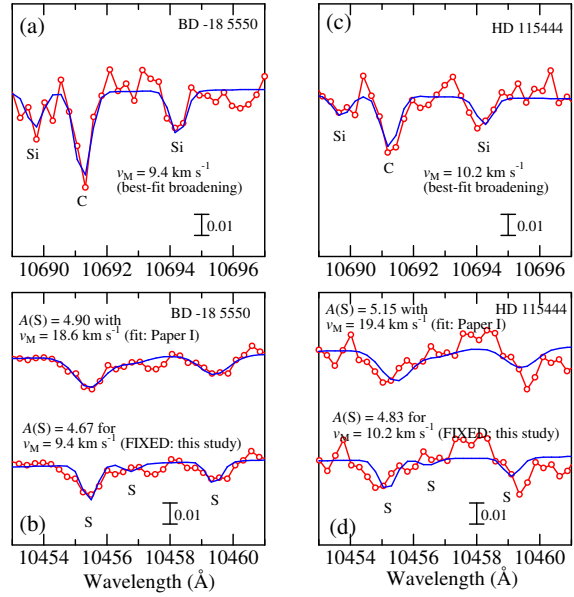


Fig. 4. Reanalysis of two stars (BD-18 5550 and HD 115444 in the left and right panels, respectively) which showed particularly high $[S/Fe]$ values in Paper I, in order to demonstrate how the choice of v_M (macrobroading parameter) influences the resulting sulfur abundance derived from spectrum fitting. Upper panels (a) and (c) ... Derivation of best-fit v_M from the C+Si feature at $\sim 1.069 \mu\text{m}$. Lower panels (b) and (d) ... Determination of $A(S)$ with two kinds of v_M treatments, where v_M is varied as an adjustable parameter (upper spectrum; method adopted in Paper I) or v_M is fixed at the value derived from the C+Si feature (lower spectrum).

abundances from the S I 10455–10459 lines while *fixing* the v_M values at the values derived from the C+Si feature, and obtained $A(S)$ values (4.67 and 4.83), which are appreciably lower than the results in Paper I (4.90 and 5.15) by 0.23 dex and 0.32 dex for BD-18 5550 and HD 115444, respectively (cf. figures 4b and 4d). We thus consider that the $[S/Fe]$ values of these two stars reported in Paper I should be revised downward by these amounts, which eventually makes +0.53 (BD-18 5550) and +0.34 (HD 115444); i.e., being almost within the $[S/Fe]$ range concluded in this study.

The star G 64-37 was actually an object of special attention, since the S abundance (based on S I 10455–10459) derived in Paper I turned out appreciably higher (by ~ 0.6 dex) than Nissen et al.’s (2007) result (based on S I 9212/9228/9237) only for this extremely metal-poor star, despite that a good agreement is seen for other comparatively more metal-rich stars; this fact motivated us to include this star again in our target list. Unlike the case of BD-18 5550 and HD 115444, a serious mismatch of v_M was not found in the analysis of Paper I. Instead, we consider that the essential problem was the comparatively poor S/N ratio (~ 100) of the spectrum used in Paper I, which is evidently insufficient for a reliable abundance de-

$v_{\text{ip}}^2 + v_{\text{mt}}^2 + v_{\text{rt}}^2$. Under this approximation, v_{ip} is evaluated as $v_{\text{ip}} = \text{FWHM}/(2\sqrt{\ln 2}) \sim 9 \text{ km s}^{-1}$ (FWHM $\sim 15 \text{ km s}^{-1}$ for $R \sim 20000$). Then, we may expect that v_{mt} would be as small as $\sim 2 \text{ km s}^{-1}$ according to the relation $v_{\text{mt}} \simeq 0.4\zeta_{\text{RT}}$ (cf. footnote 12 of Takeda et al. 2008) since the typical ζ_{RT} (radial-tangential macroturbulence) is $\sim 5 \text{ km s}^{-1}$ for early G dwarfs and early-K giants (cf. figure 17.10 in Gray 2005). Finally, we may regard that v_{rt} ($\simeq 0.94v_e \sin i$; cf. footnote 12 of Takeda et al. 2008) is of minor importance (e.g., presumably no larger than $\sim 2\text{--}3 \text{ km s}^{-1}$ in most cases), since the stellar rotation must have been spun down in these old halo stars. Accordingly, v_M is reasonably expected to be around $\sim 10 \text{ km s}^{-1}$, because it is primarily determined by the contribution from v_{ip} .

⁶ For the other stars, both $A(S)$ and v_M were varied to determine as in Paper I. However, we checked for each star that the resulting $v_M(S)$ (cf. table 1) is not in serious disagreement with v_M (C+Si). Note that HD 195636 is a rather unusual star, since

its v_M (17.0 km s^{-1}) is appreciably large (an alternative C+Si fitting also yielded a similar result), which might have a comparatively high $v_e \sin i$ for stars of this class.

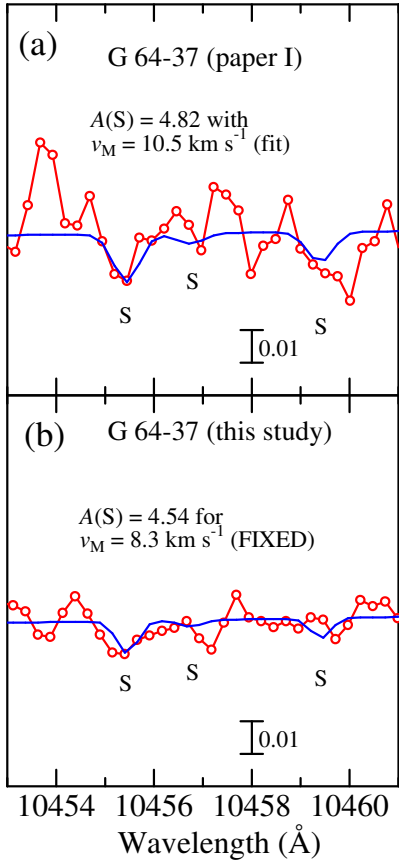


Fig. 5. Comparison of the spectra and the $A(S)$ determination procedures for G 64-37, for which two independent analyses were performed in Paper I (based on the 2009 data) as well as in this study (based on the 2011 data).

termination from very weak lines with depression on the order of $\sim 1\%$. The observed and the fitted spectrum in Paper I and those in this study are compared in figure 5. We can see from this figure that the previous analysis was severely influenced by the large noise, while the situation has been improved in present case ($S/N \sim 200$), resulting in an appreciable difference of solution between the two cases. We naturally consider the present result of $A(S) = 4.54$ ($[S/Fe] = +0.42$) is more credible than that in Paper I, requiring a downward revision of the previous $[S/Fe]$ value (+0.69) by -0.27 dex, by which the disagreement with Nissen et al. (2007) has been reasonably mitigated by this amount.

5. Conclusion

This study was motivated by the recent extensive work done by Spite et al. (2011) who reported that $[S/Fe]$ ratios of very metal-poor stars determined from the S I 9212/9228/9237 lines show a nearly flat behavior at a mildly supersolar level of $\sim +0.2$ – 0.5 over a wide metallicity range of $-3.5 \lesssim [Fe/H] \lesssim -2$, which markedly contradict the conclusion of our previous study based on S I

10455–10459 lines (Paper I) that such a flat tendency of $[S/Fe]$ (persisting down to $[Fe/H] \sim -2.5$) is followed by a sudden jump up to $+0.7$ – 0.8 around $[Fe/H] \sim -3$.

With an intention to resolve the cause of this discrepancy, we rechallenge the task of clarifying the $[S/Fe]$ ratios at the extremely low metallicity regime down to $[Fe/H] \sim -3$ by using the same triplet lines as used in Paper I, based on the new observational data for an extended sample of 13 very metal-poor stars observed with IRCS+AO188 of the Subaru Telescope.

In almost the same manner as in Paper I, we conducted a non-LTE spectrum fitting analysis of S I 10455–10459 triplet, and found that the resulting $[S/Fe]$ values were moderately supersolar uniformly scattering around $\sim +0.3$ – 0.4 [with the mean abundance of $\langle [S/Fe] \rangle = +0.34$ ($\sigma = 0.16$)] over $-3.2 \lesssim [Fe/H] \lesssim -1.9$ without any systematic $[Fe/H]$ -dependence, which confirmed the consequence corroborated by Spite et al. (2011) based on the S I 9212/9228/9237 lines.

Given these new observational facts, we reexamined the process of our previous analysis for the three extremely metal-poor stars (G 64-37, BD–18 5550, and HD 115444), for which we derived prominently high $[S/Fe]$ values ($\sim +0.7$ – 0.8) that eventually lead to the conclusion of Paper I. Regarding G64-37, our reanalysis using a new spectrum of higher quality yielded a result lower than the previous value by ~ 0.3 dex. For BD–18 5550 and HD 115444, we noticed that our automatic profile-fitting method (which varies both the abundance and the broadening parameter to find the best fit) resulted in unreasonably large solutions of the broadening width, because of the considerable weakness of the line profile severely damaged by noises. When the broadening parameter was fixed at the more reasonable values determined from stronger lines, we found that the revised solution of the S abundance is lowered by ~ 0.3 – 0.4 dex for both of these stars. Consequently, it is likely that we had overestimated the $[S/Fe]$ values of these three stars in Paper I by ~ 0.3 – 0.4 dex.

Accordingly, we now consider that the flat trend of $[S/Fe]$ (without any systematic rise with a decrease of metallicity) represents the truth, at least with regard to the overall $[S/Fe]$ behavior of very metal-poor stars in general, which means the withdrawal of our previous argument that $[S/Fe]$ experiences a sudden jump up to conspicuously large $[S/Fe]$ of $\sim +0.8$ as the metallicity is lowered down to the $[Fe/H] \sim -3$ regime.

We finally remark, however, that the existence of some stars deviating from the main trend with appreciably higher/lower $[S/Fe]$ amounting to $[S/Fe] \sim +0.7/0.0$ as a result of the natural diversity is not necessarily be excluded (e.g., we derived $[S/Fe] = +0.66$ for HD 126587 and $[S/Fe] = -0.01$ for HD 13979). Actually, since our 13 stars (at $[Fe/H] \lesssim -2$) yielded $\langle [S/Fe] \rangle = +0.34$ with σ (standard deviation) of 0.16, we may expect the probability of finding $\geq 1\sigma$ deviation ($[S/Fe] \lesssim +0.2$ or $[S/Fe] \gtrsim +0.5$) and $\geq 2\sigma$ deviation ($[S/Fe] \lesssim 0.0$ or $[S/Fe] \gtrsim +0.7$) to be

$\sim 30\%$ and $\sim 5\%$, respectively.⁷ From this point of view, the recent Koch and Caffau's (2011) result of $[S/Fe]$ as somewhat high as $\sim +0.5$ for a red giant in the very metal-poor globular cluster NGC 6397 ($[Fe/H] \sim -2.1$) may be understandable without invoking a bimodal $[S/Fe]$ trend such as they discussed.

We express our heartfelt thanks to T.-S. Pyo and Y. Minowa for their kind advices and helpful support in preparing as well as during the IRCS+AO188 observations.

One of the authors (M. T.-H.) is grateful for a financial support from a grant-in-aid for scientific research (C, No. 22540255) from the Japan Society for the Promotion of Science.

This research has made use of the SIMBAD database, operated by CDS, Strasbourg, France.

References

- Burris, D. L., Pilachowski, C. A., Armandroff, T. E., Sneden, C., Cowan, J. J., & Roe, H. 2000, *ApJ*, 544, 302
- Carney, B. W., Latham, D. W., Stefanik, R. P., Laird, J. B., & Morse, J. A. 2003, *AJ*, 125, 293
- Cayrel, R. 1988, in *Proc. IAU Symp. 132, The Impact of Very High S/N Spectroscopy on Stellar Physics*, ed. G. Cayrel de Strobel & M. Spite (Dordrecht: Kluwer), 345
- Frebel, A., Christlieb, N., Norris, J. E., Thom, C., Beers, T. C., & Rhee, J. 2007, *ApJ*, 660, 117
- Gray, D. F. 2005, *The Observation and Analysis of Stellar Photospheres*, 3rd ed. (Cambridge: Cambridge University Press)
- Hansen, C. J., & Primas, F. 2011, *A&A*, 525, 5
- Ishigaki, M., Chiba, M., & Aoki, W. 2010, *PASJ*, 62, 143
- Jönsson, H., Ryde, N., Nissen, P. E., Collet, R., Eriksson, K., Asplund, M., & Gustafsson, B. 2011, *A&A*, 530, A144
- Koch, A., & Caffau, E. 2011, *A&A*, 534, A52
- Kurucz, R. L., Furenlid, I., Brault, J., & Testerman, L. 1984, *Solar Flux Atlas from 296 to 1300 nm* (Sunspot, New Mexico: National Solar Observatory)
- Nissen, P. E., Akerman, C., Asplund, M., Fabbian, D., Kerber, F., Käuff, H. U., & Pettini, M. 2007, *A&A*, 469, 319
- Rich, J. A., & Boesgaard, A. M. 2009, 701, 1519
- Saito, Y.-J., Takada-Hidai, M., Honda, S., & Takeda, Y. 2009, *PASJ*, 61, 549
- Spite, M., et al. 2011, *A&A*, 528, A9
- Takeda, Y. 1995, *PASJ*, 47, 287
- Takeda, Y., Hashimoto, O., Taguchi, H., Yoshioka, K., Takada-Hidai, M., Sato, Y., & Honda, S. 2005, *PASJ*, 57, 751
- Takeda, Y., Sato, B., & Murata, D. 2008, *PASJ*, 60, 781
- Takeda, Y., & Takada-Hidai, M. 2011, *PASJ*, 63, S537 (Paper I)

⁷ This estimation naturally depends on the extent of σ . We note that the $\sigma([S/Fe])$ of $[Fe/H] \leq -2$ stars derived by other investigators are somewhat smaller than our result; e.g., $\sigma = 0.07$ (Nissen et al. 2007), $\sigma = 0.12$ (Spite et al. 2011), $\sigma = 0.11$ (Jönsson et al. 2011). It should thus be important to quantitatively establish not only the trend of $[S/Fe]$ on the average but also the extent of its dispersion based on a large sample of very metal-poor stars.

Table 1. Parameters of the program stars and the results of abundance analyses.

Name	T_{eff} (K)	$\log g$ (cm s^{-2})	v_t (km s^{-1})	[Fe/H] (dex)	Ref.	v_M (km s^{-1})	A^N (dex)	EW_{10455} (mÅ)	Δ_{10455} (dex)	[S/Fe] (dex)	S/N	Remark
CS 30323-048	6338	4.32	1.5	-3.21	NIS07	(8.7)	4.29	2.8	-0.25	+0.30	350	v_M fixed, larger uncertainty
HD 126587	4700	1.05	1.7	-3.16	HAN11	(12.7)	4.70	14.2	-0.27	+0.66	300	v_M fixed
G 206-34	5825	3.99	1.5	-3.12	RIC09	(9.4)	4.55	3.6	-0.19	+0.47	450	v_M fixed
G 64-37	6432	4.24	1.5	-3.08	NIS07	(8.3)	4.54	5.5	-0.26	+0.42	200	v_M fixed
HE 1523-0901	4630	1.00	2.6	-2.95	FRE07	(10.3)	4.42	6.7	-0.19	+0.17	350	v_M fixed
BD-16 251	4825	1.50	1.8	-2.91	AND10	9.4	4.64	10.2	-0.23	+0.35	450	
HD 195636	5370	2.40	1.5	-2.77	CAR03	17.0	4.88	19.1	-0.35	+0.45	300	large v_M (cf. footnote 5)
G 186-26	6417	4.42	1.5	-2.54	NIS07	12.0	5.02	10.7	-0.15	+0.36	500	
HD 186478	4730	1.50	1.8	-2.42	HAN11	13.3	5.19	22.8	-0.19	+0.41	350	
HD 6268	4735	1.61	2.1	-2.30	SAI09	9.5	5.20	21.4	-0.17	+0.30	450	
HD 13979	5075	1.90	1.3	-2.26	BUR00	11.8	4.93	16.6	-0.21	-0.01	450	
HD 221170	4560	1.37	1.6	-2.00	SAI09	9.2	5.49	28.7	-0.16	+0.29	200	
HD 216143	4525	1.77	1.9	-1.92	SAI09	9.4	5.50	19.9	-0.10	+0.22	550	
Vesta (Sun)	5780	4.44	1.0	0.00	...	10.7	7.21	123.5	-0.09	+0.01	600	

In columns 1 through 6 are given the star designation, effective temperature, logarithmic surface gravity, microturbulent velocity dispersion, Fe abundance relative to the Sun, and key for the reference of atmospheric parameters: BUR00 ... Burris et al. (2000), CAR03 ... Carney et al. (2003), FRE07 ... Frebel et al. (2007), HAN11 ... Hansen and Primas (2011), NIS07 ... Nissen et al. (2007), RIC09 ... Rich and Boesgaard (2009), SAI09 ... Saito et al. (2009). Columns 7–11 present the results of the abundance analysis based on the S I 10455–10459 profile-fit: v_M is the best-fit macrobroadening parameter (while those in parentheses are the assumed or fixed values, which were separately derived from the C+Si 1.069 μm feature fitting), A^N is the non-LTE logarithmic abundance of S (in the usual normalization of H = 12.00) derived from spectrum-synthesis fitting, EW_{10455} is the equivalent width (in mÅ) for the S I 10455 line inversely computed from A^N , Δ_{10455} is the non-LTE correction ($\equiv A^N - A_{10455}^L$) for the S I 10455 line, and [S/Fe] ($\equiv A^N - 7.20 - [\text{Fe}/\text{H}]$) is the S-to-Fe logarithmic abundance ratio relative to the Sun. The S/N ratio of the spectrum estimated at the position of the S I lines is given in column 12. The objects are arranged in the ascending order of [Fe/H].